Desalination and Water Treatment
www.deswater.com

doi: 10.5004/dwt.2019.23939

152 (2019) 234–241
June

Removal of Ochratoxin A from water by novel adsorbent; magnetic carbon nanocomposites prepared from sugar beet wastes

Muhammad Zahoor[a,*], Naila Gulfam[b], Muhammad Khisroon[b], Farhat Ali Khan[c]

[a]*Department of Chemistry, University of Malakand, Chakdara, Dir Lower, 18800 KPK, Pakistan, email: mohammadzahoorus@yahoo.com*
[b]*Department of Zoology, Peshawar University, Khyber Pakhtunkhwa, Pakistan, emails: nailazoo@yahoo.com (N. Gulfam), m_khisroon@upesh.edu.pk (M. Khisroon)*
[c]*Principal Abbotabad International College of Pharmacy AIMI, Abbotabad, KPK, Pakistan, email: farhatkhan2k9@yahoo.com*

Received 27 August 2018; Accepted 11 February 2019

ABSTRACT

In this study, a novel adsorbent, magnetic carbon nanocomposite, was prepared from sugar beet wastes and was used for the in vitro detoxification of ochratoxin A. The prepared adsorbent was characterized by surface area analyzer, scanning electron microscopy, x-ray diffraction, energy dispersive x-ray, thermal gravimetric/differential thermal analysis and fourier transform infrared. Freundlich, Temkin and Langmuir isotherms were used to determine the adsorption parameters of the ochratoxin A adsorption. Pseudo-first and pseudo-second order kinetic models were used to determine the kinetic parameters of the adsorption process. Langmuir isotherm and pseudo-first order kinetic model fitted well the experimental data. The equilibrium time at pH 7 was 235 min. The effect of pH on adsorption of ochratoxin A was also determined. A slight decline in percent adsorption from pH 1 to 13 was observed. The thermodynamic parameters were also determined. The value of $\Delta S°$ (85 kJ.mol^{-1}.deg^{-1}) was positive while the values of $\Delta H°$ (–21 kJ mol^{-1}) and $\Delta G°$ (–2.75, –3.57, –4.39 and –5.21 kJ mol^{-1} at 30°C, 40°C, 50°C and 60°C, respectively) were negative. The negative value $\Delta H°$ indicates the exothermic nature of the process while the increased negative values of $\Delta G°$ at high temperature showed the favorable nature of process at high temperature. From the results, it was concluded that this adsorbent could be used as alternative of activated carbon for the detoxification of ochratoxin A both in poultry feed and in gastrointestinal tract of broilers.

Keywords: Ochratoxin A; Sugar beet waste; Nanocomposite

1. Introduction

In poultry feeds, ochratoxins are produced by certain fungi especially when the environmental conditions are favorable. They badly affect poultry birds and human health. Amongst the ochratoxins, ochratoxin A contamination in poultry feed is ubiquitous [1]. Ochratoxin A in poultry feed is produced by *Aspergillus ochraceus*, *Aspergillus niger*, *Aspergillus carbonarius* and *Penicillium verrucosum* [2].

Various chemical, physical and biological methods are used for the detoxification of ochratoxins [3]. Different adsorbents are used for the detoxification of ochratoxin A in poultry feed as well as gastrointestinal tract of poultry birds. The adsorbents bind the ochratoxin A in the gastrointestinal tract of chicks and then excreted with faeces without producing any injurious effects [4]. Due to safety and feasibility to mix in poultry feed, low price and high efficacy in detoxification of mycotoxins, the use of adsorbent is preferred over the other methods. The adsorbents that have been used for the adsorption of mycotoxin in poultry feed and gastrointestinal tract of poultry birds include aluminosilicate, bentonite, zeolite and activated charcoal [4].

Activated carbon due to its high surface area is widely used for the removal of organic and inorganic contaminants

* Corresponding author.

from water. However, due to its light weight, their settling time in reactors is high; the important factor in the recovery of adsorbent after use. To remove this discrepancy, a number of authors have attempted to make it magnetic which can then be easily removed from slurry after treatment through the magnetic process. Magnetic oxides and magnetic carbon nanocomposites have been used in removal of various organic and inorganic contaminants from water by a number of researchers [4–6]. These adsorbents have magnetic character due to which they can easily be collected from slurry after use through magnetic process [4]. However when magnetic oxides are deposited on activated carbon there is a considerable decrease in the surface area of the resulting composite [4,7–9]. Thus there is a need to prepare such adsorbent having a magnetic character with the high surface area.

In order to solve the above-mentioned problem, the current study was aimed to prepare highly porous magnetic nanocomposites from sugar beet waste and to evaluate its efficacy for the detoxification of ochratoxin A.

2. Material and methods

2.1. Preparation and characterization of highly porous carbon based nanocomposites

The novel adsorbent was prepared using a method devised by Zahoor and Khan [4] with slight modification. The dried waste biomass was crushed and soaked in ethanolic $FeCl_3.6H_2O$ (10% w/v). After 30 min, the biomass was taken out and dried for 24 h at room temperature. The dried mass was then kept in oven for 5 h at 100°C. The dried mass was then charred in the continuous supply of nitrogen gas at 500°C in a specially designed chamber. The charred material was kept in the chamber for 2 h at the same temperature to accomplish the process. A magnetic bar was used to find out whether the resulting mass has magnetic character or not. All the sample contents stick to magnet bar indicating that iron oxide is present on the surface of the prepared composite. To enhance porosity, the prepared adsorbent was treated with different concentrations HNO_3 solutions for 75 min. HNO_3 treatment caused the detachment of iron oxide from composite surface. Complete removal of iron oxide from the composite surface was caused by concentrated HNO_3 solutions. However partial removal of iron oxide was observed with diluted solutions and 0.01 N HNO_3 was found optimum at which 50% of the iron oxide contents were intact which was desirable for magnetic applications.

The prepared magnetic carbon nanocomposites were then characterized by different instrumental techniques such as surface area analyzer (Anton Paar, USA), scanning electron microscopy (SEM), x-ray diffraction (XRD), energy dispersive x-ray (EDX), thermal gravimetric/differential thermal analysis (TG/DTA) and fourier transform infrared (FTIR).

The surface area of novel adsorbent was determined using NovaWin instrument version-11.04 type surface area analyzer, Quantachrome. For SEM analyses, the sample was put on SEM on grid and gold coated through sputter coater (SPI, USA) at 30 mA for 2 min. JSM-5910 (JEOL) type SEM machine was used for taking the images of the sample at an accelerating voltage of 20 kV.

JEOL X-ray diffractometer (JDX-3532) was used to confirm the magnetic character of the sample. The detailed operations conditions were current = 2.5–80 mA, voltage = 20–60 kV, X-rays = Cu Kα, 2θ = –3° to 160°. The machine was equipped with a Ni filter. Using monochromatic Cu Kα radiation of 1.5418Å wavelength, scanning range 2θ/θ and scanning speed 10 min^{-1} to draw X-ray diffractogram of the sample.

The elemental composition was determined through SEM JSM-5910 (JEOL, Japan) model INCA 200 X-sight Oxford Instrument UK. The sample particles were spread on both sides of adhesive tape which was then placed on microscope stub.

Diamond Series TG/DTA (PerkinElmer, USA) analyzer was used to determine the mass loss with an increase in temperature using Al_2O_3 as reference standard.

IR Prestige-21, Shimadzu, Japan, machine was used to draw FTIR spectra of the sample in the range of 750–525 cm^{-1} and 4,000–600 cm^{-1}.

2.2. Determination of kinetic parameters

To a series of 25 mL flasks, 5.4 mL ethanol and 13 mL distilled water (pH 7) were added. Each flask was spiked with a known quantity of standard ochratoxin A (200 ppm). Then the prepared adsorbent was put into these flasks in such a way to attain 0.5% w/v concentration of adsorbent in each flask. Rotation of these flasks was carried at 300 rpm for 450 min at room temperature. Separation of sorbents was done using bar magnet and Whatman No 1 filter paper prior to high performance liquid chromatography (HPLC) analyses.

2.2.1. Ochratoxin quantification by HPLC

Quantification of ochratoxin A was carried out using a HPLC system (Hitachi model L-200) with two pumps L-2130, automobile injector L-2200 and fluorescence detector L-2458 (Macau, Japan). Through sonication degassing of the mobile phase (acetonitrile/methanol/normal water at the ratio of 8:27:65, v/v/v) was carried out. The column inertsil ODS-3 (25 cm × 4.5 mm I.D., 5 nm, GL knowledge, Tokyo, Japan) was linked as LC column and retained at 40°C. The injecting volume was 20 μL with a rate of flow of 0.8 mL/min. The ochratoxin A was detected at the wavelengths of 365 and 450 nm (excitation and emission), respectively.

2.3. Determination of adsorption parameters

In a series of flasks, 150, 175, 200, 225, 250, 275, 300, 325 and 350 ppm solutions of ochratoxin A were taken. To all of them, the novel adsorbent was added in such a way to attain 0.5% w/v concentration of adsorbent in each flask. All the flasks were then shaken at 300 rpm for 450 min at room temperature. After separation of adsorbent, the solutions were subjected to HPLC analysis as described above.

2.4. Determination of effect of pH on adsorption

In a series of 25 mL flasks 200 ppm ochratoxin A solutions were taken. The pH in these flasks was adjusted (1–14) using NaOH and HCl. Then adsorbent was added to each flask and all the flasks were rotated at 300 rpm for 450 min. The sorbent was then separated from the slurry and LC analysis was carried out as described above.

2.5. Effect of temperature on adsorption

Four flasks (50 mL) were taken and 200 ppm solutions of ochratoxin A was poured in each flask. To each flask magnetic nanocomposite were added and were shaken at 30°C, 40°C, 50°C and 60°C for 450 min. The adsorbent was then separated from the slurry through bar magnet and subjected to HPLC analysis as described above.

2.6. Regeneration of ochratoxin A loaded adsorbent

About 0.15 gram was thoroughly shaken 50 mL of 200 ppm solution of ochratoxin at room temperature and 300 rpm for 6 h. The un-adsorbed ochratoxin A in the supernatant was determined through HPLC. The ochratoxin-loaded adsorbent was isolated from the reaction mixture using a magnet bar. The prepared carbon nanocomposites were regenerated by washing for five times with 3% NaOH solution, methanol and distilled water.

3. Results and discussion

3.1. Characterization of nanomaterials

Table 1 shows various surface parameters of the novel adsorbent. The BET surface area of the composite was 198.40 m^2/g with a total pore volume of 3.02 cm^3/g, a micro pore volume of 1.12 cm^3/g and 71.45 Å average pore diameter.

The SEM images of composite (Fig. 1(a)) show white patches on the surface which confirms the presence of iron oxide that has been deposited in the pores of the composite, whereas the black portion represents the carbon.

In the present study, an attempt was made to enhance the porosity of the prepared composites by treating it with different concentration HNO_3 solution for 75 min. Amongst them, treatment with 0.01 N HNO_3 solution was found optimum and at this concentration 50% iron oxide contents were left there intact on composite surface. This treatment was done to enhance the porosity of the composite as the deposition of iron oxide on composite surface results in the reduction of surface area and blocks the pores. The presence of intact iron oxide in a composite structure is desirable for magnetic applications. However, too much iron oxide deposition results in pore blocking which considerably reduces the surface area of the composite. Fig. 1(b) shows an overview of the iron oxide carbon nanocomposite after treating with HNO_3. The enhanced porosity is evident from its honeycomb-like porous surface which confirms that the excess of deposited iron oxide has been removed by HNO_3.

The XRD spectrum of highly porous carbon nanocomposites is presented in Fig. 1(c). The XRD analysis shows diffraction peaks at 2θ; 16.05, 35.55 and 62.6 representing the corresponding indices; 111, 311 and 440 of magnetite [4,8]. Diffraction peaks at 2θ; 11.85, 19.40, 25.15, 33.15, 40.5, 45.05 and 54.05 correspond to indices; 020, 110, 120, 130, 121, 131 and 221 of goethite [10,11]. The diffraction peaks at 2θ; 24.2 and 49.5 corresponding to indices of 012 and 024 representing hematite [9].

Table 1
Surface characteristics of carbon nanocomposites

Physical properties	Values	Units
BET surface area	198.40	m^2/g
Langmuir surface area	877.14	m^2/g
Total pores volume	3.03	cm^3/g
Micro pore volume	1.12	cm^3/g
Average pore diameter	71.45	Å

According to Al-Qodah and Shawabkah [12], the disappearance of iron oxide takes place if the iron oxide carbon nanocomposites are treated with concentrated HNO_3 solution. However, in our study, the total removal of the iron oxide was not desired; therefore, the composite was treated with dilute acid solutions.

EDX image of highly porous carbon nanocomposite is shown in Fig. 1(d). The existence of iron and oxygen evident at different keV. The Fe peaks are present at 0.8, 6.4 and 7 keV whereas the oxygen peak can be found at 0.4 keV.

The TG/DTA analysis has been shown in Fig. 1(e). There is a slight decrease in mass near 100°C after which the mass of the sample remained constant up to 390°C and then rapid fall in the weight can be observed from 420°C to 560°C. The mass loss from 390°C to 420°C is slow, whereas beyond 420°C sudden fall in weight can be observed and there is no farther loss in mass after 560°C. In DTA curve, two endothermic peaks along with exothermic peaks can be observed.

Figs. 1(f) and (g) show the IR spectra of prepared adsorbent. The bands at 3,380 and 2,660 cm^{-1} were assigned to O–H and aliphatic C–H groups, respectively. The bands of C=O and C=C were observed at 1,200 to 1,000 cm^{-1} [12]. The bands at 1,004.91 and 1,180 cm^{-1} were assigned to C–O bond stretching [13] whereas band at 595 cm^{-1} correspond to stretching of Fe–O of the deposited iron oxide of the composite surface [14].

3.2. Adsorption isotherm

Giles isotherm [15] was obtained by plotting concentration (C) vs. amount of ochratoxin A adsorbed (q) (Fig. 2(a)). Isotherms in Fig. 2 are C type which is characterized by the constant partition of contaminant between solution and substrate up to maximum possible adsorption. It also indicates that the number of the adsorption sites remains constant and with the advancement of adsorption process more sites are constantly produced that is evident from the linearity of the curve.

Langmuir [16], Freundlich [17] and Temkin adsorption isotherms [18] were used to quantify the adsorption potential of ochratoxin A on the prepared adsorbent. The linear form of Langmuir isotherm is given as follows:

$$\frac{C}{q} = \frac{C}{Q_0} + \frac{1}{Q_0 b} \tag{1}$$

In this equation, the amount of ochratoxin A adsorbed (mg g^{-1}) is represented by q, the equilibrium concentration of ochratoxin A (mg L^{-1}) is represented by C, whereas b and Q_0 are constants relating to an energy of the process and maximum adsorption capacity of the adsorbent. The plots of equilibrium concentration (C) against specific adsorption (C/q) is presented in Fig. 2(b). The values of Langmuir

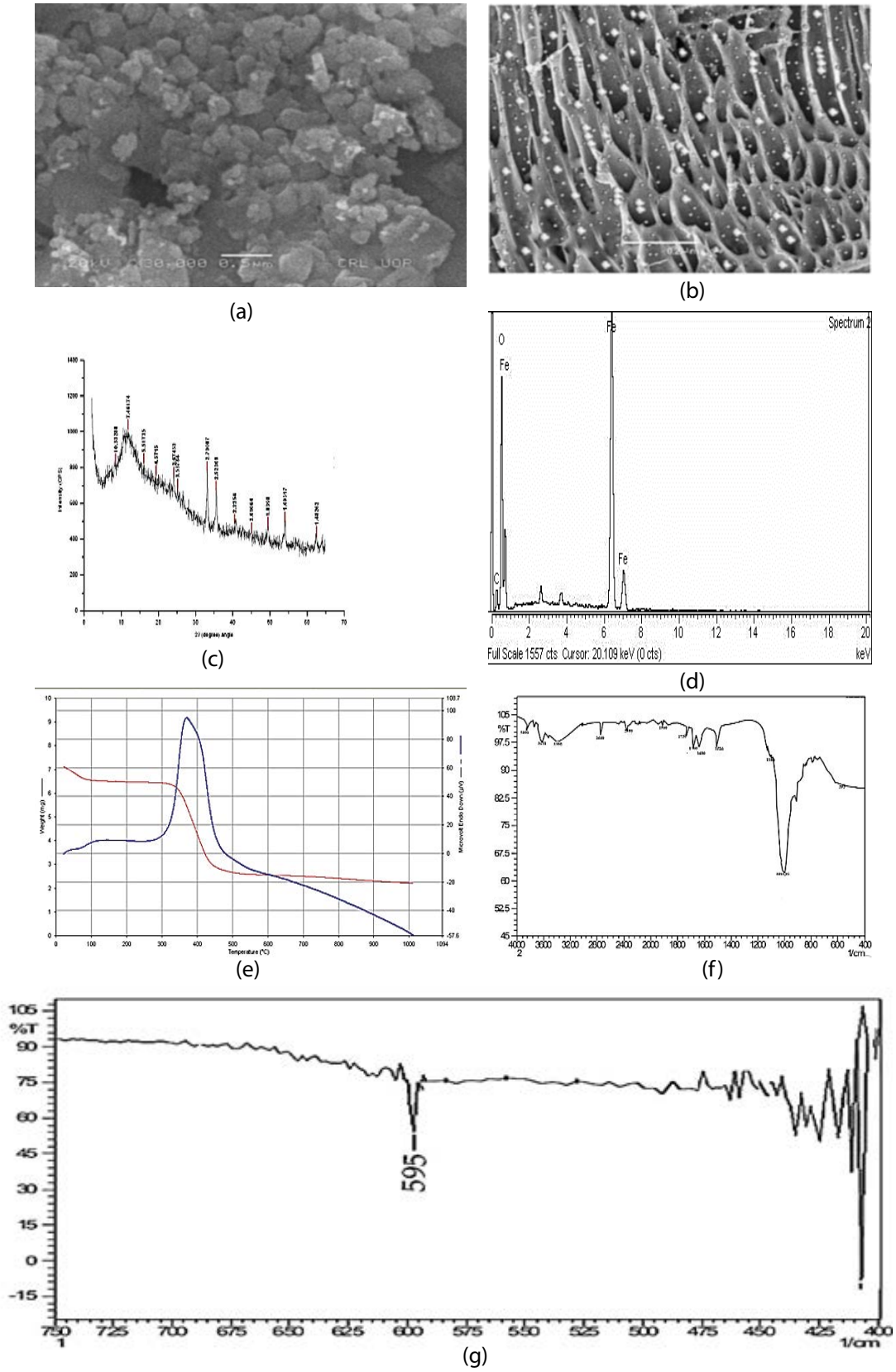

Fig. 1. Instrumental characterization of the prepared iron oxide carbon nanocomposites prepared from sugar beet waste. (a) Before HNO_3 treatment, (b) after HNO_3 treatment, (c) XRD pattern of adsorbent, (d) EDX spectra, (e) TG/DTA analysis, (f) FTIR spectra (far region) and (g) FTIR spectra (med region).

constants b and Q_0 were calculated from the slope and intercept of the plot and were found to be 0.072 and 347.2 mg g^{-1}, respectively (R^2 = 0.995).

The heterogeneous systems are generally described well by Freundlich isotherm. The Freundlich isotherm equation is presented as follows:

$$\ln q = \ln K + \frac{1}{n}\ln C \tag{2}$$

C represents the equilibrium concentration (mg L^{-1}), the total amount of ochratoxin A adsorption (mg g^{-1}) is represented by q while K and n are constants showing the adsorption capacity and the intensity of the adsorption, respectively.

The values of Freundlich constants K and $1/n$ were calculated from the slope and intercept of the ln$C$ vs. ln$q$ plot (Fig. 2(c)) and were found to be 26.5 and 0.876, respectively, with R^2 value of 0.990 (Table 2).

Usually, the following linear form of Temkin isotherm is applied to explain the equilibrium adsorption data [18].

$$q_e = \beta \ln \alpha + \beta \ln C_e \tag{3}$$

In Eq. (3), $\beta = RT/b$, T = absolute temperature in Kelvin and R = general gas constant. The value R is 8.314 J mol^{-1} K^{-1}. When q_e was plotted against ln C_e, a straight line was obtained (Fig. 2(d)). From slope and intercept, the values of β and $\beta \ln\alpha$ were calculated (Table 2).

From Table 2, it is clear that Langmuir adsorption isotherm fitted the data well as compared with Freundlich and Temkin isotherm as the R^2 value for this model is high.

3.3. Adsorption kinetics

Fig. 2(e) shows time t vs. C plot of ochratoxin A (200 ppm) adsorption on prepared adsorbent at pH 7. After some time most of the free sites are filled up by ochratoxin A. As a result, the rate of adsorption slows down. Finally, a point is reached at which the rate of adsorption and desorption become equal which is an adsorption equilibrium point. From the graph, the adsorption equilibrium was found to be 235 min.

The adsorption kinetics data were analyzed using pseudo-first and pseudo-second order [19,20] adsorption kinetic models. The linear form of pseudo-first order model is given as follows:

$$\ln\left(q_e - q\right) = \ln q_e - k_a t \tag{4}$$

In the above equation, q_e represents the amount of ochratoxin A adsorbed (mg g^{-1}) at equilibrium whereas q is the amount of ochratoxin A adsorbed (mg g^{-1}) at time t and k_a (min^{-1}) is the first order rate constant. The plot of $1n(q_e - q)$ against t is shown in Fig. 2(f). The values of k_a and R^2 were found to be 0.0188 and 0.990, respectively.

The linear form of pseudo-second order kinetics model is given as follows:

$$\frac{t}{q_t} = \frac{1}{k_2 q^2} + \left(\frac{1}{q}\right)t \tag{5}$$

A straight line was obtained, when t/q was plotted against t (Fig. 2(g)). The values K_2 and q were obtained from intercepts and slopes of the plot and their values are presented in Table 3.

Pseudo-first order model fitted the experimental data well as compared with pseudo-second order kinetic model which was evident from their R^2 values (Table 3).

3.4. Effect of pH

The influence of pH on ochratoxin A adsorption is shown in Fig. 3(a). There is a slight decrease in %adsorption from pH 1 to 13. At acidic pH, the high adsorption capacity of the adsorbent can be explained on the basis of two important factors: (i) At acidic pH the deposited iron oxide detaches from the surface that causes an increase in surface area consequently that results in high adsorption capacity while at basic pH, the iron oxide remains intact on the surface of the composite, therefore, there is a slight decrease in percent adsorption. (ii) At acidic pH, the deprotonation of the OH^- group (depicted in FTIR spectra) of adsorbent and the three ionizable group present in the structure of ochratoxin A is suppressed (Fig. 3(b)) resulting in positive interactions. From pH 1 to 5.70 the ochratoxin A molecule is neutral. At basis pH deprotonation of both adsorbent and adsorbate takes place. Thus negative interactions lower the adsorption rate.

3.5. Adsorption thermodynamics

For the calculation of thermodynamics parameters, adsorption experiment was performed at a different temperature (30°C, 40°C, 50°C and 60°C). The values of $\Delta H°$ and $\Delta S°$ were calculated from Van't Hoff equation, given as follows:

$$\ln k = \frac{\Delta S^\circ}{R} - \frac{\Delta H}{RT} \tag{6}$$

In the above equation, K is the distribution constant of adsorption, $\Delta H°$ represents the enthalpy change while the entropy change is denoted by $\Delta S°$. R is universal gas constant and T is temperature (Kelvin). $\Delta H°$ value was calculated from the slope whereas the value of $\Delta S°$ was determined from the intercept of the InK and $1/T$ plot (Fig. 3(c)) and were found to be –21 kJ mol^{-1} and 85 kJ mol^{-1} deg^{-1}, respectively. The negative value of $\Delta H°$ shows that the adsorption of ochratoxin A on prepared adsorbent was an exothermic process. The positive value of $\Delta S°$ shows that there is an increase in the randomness in the system at the solid/solution interface.

The value of $\Delta G°$ (standard free energy) was calculated from the following equation:

$$\Delta G^\circ = \Delta H^\circ - T\Delta S^\circ \tag{7}$$

The values $\Delta G°$ were: –2.75, –3.57, –4.39 and –5.21 kJ mol^{-1} at temperature; 30°C, 40°C, 50°C and 60°C, respectively. The negative values of $\Delta G°$ show that with increase in temperature there is an increase in adsorption.

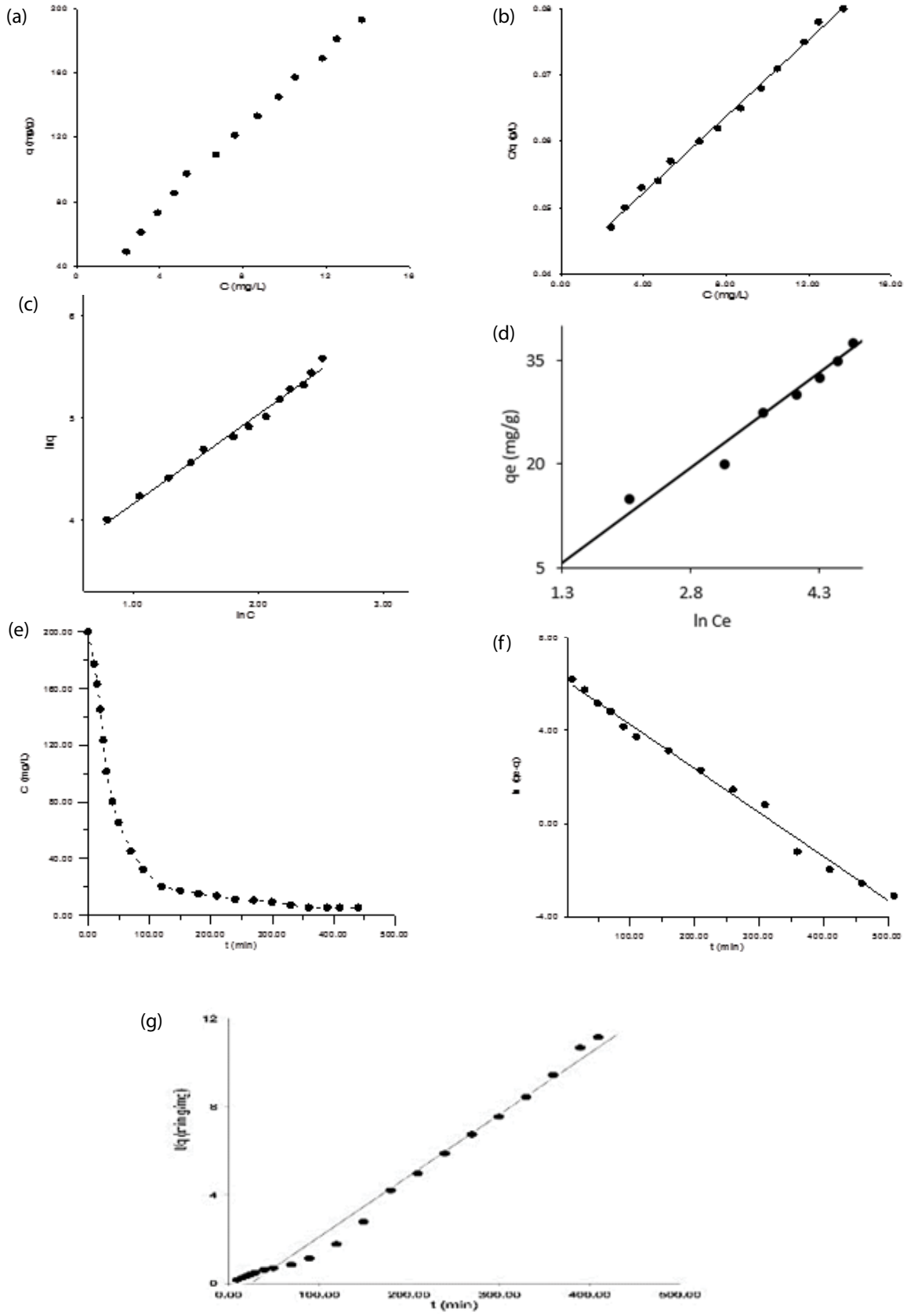

Fig. 2. Parameters of ochratoxin A adsorption. (a) Giles isotherm, (b) Langmuir isotherm, (c) Freundlich isotherm, (d) Temkin isotherm, (e) effect of contact time on adsorption, (f) pseudo-first order model and (g) pseudo-second order model.

3.6. Regeneration of the novel adsorbent

Regeneration of adsorbent is very important from economical point of view. The solid mass of adsorbent was washed with 3% NaOH solution, methanol and distilled water. The washing process was repeated for five times till the ochratoxin concentration was less than 4 ppm. The adsorbent was dried in an oven at 70°C for 150 min which was then ready for reuse again. This recycling test was conducted for about six times. During these cycles, about 2% loss in the activity were observed.

Table 2
Isotherm parameters for ochratoxin A adsorption

Langmuir isotherm			Freundlich isotherm			Temkin isotherm			
Q_0 (mg g^{-1})	b	R^2	K	1/n	R^2	b	α	β	R^2
347.2	0.072	0.995	26.5	0.876	0.990	85.6	1.84	7.24	0.972

Table 3
Pseudo-first and second order adsorption rate constants and correlation coefficients for the adsorption of ochratoxin A onto iron oxide carbon nanocomposites

Equation type	Pseudo-first order kinetics model		Equation type	Pseudo-second order kinetics model	
	K_a	R^2		K_2	R^2
Linear: $\ln(q_e - q_t) = \ln q_e - K_a t$	0.0188	0.990	Linear: $\frac{t}{q_t} = \frac{1}{k_2} + \frac{t}{q_e}$	0.00107	0.980
Non-linear: $q_t = q_e\left(1 - e^{-k_2 t}\right)$	0.0321	0.994	Non-linear: $q_t = \frac{k_2 q_e^2 t}{1 + k_2 q_e t}$	0.00176	0.972

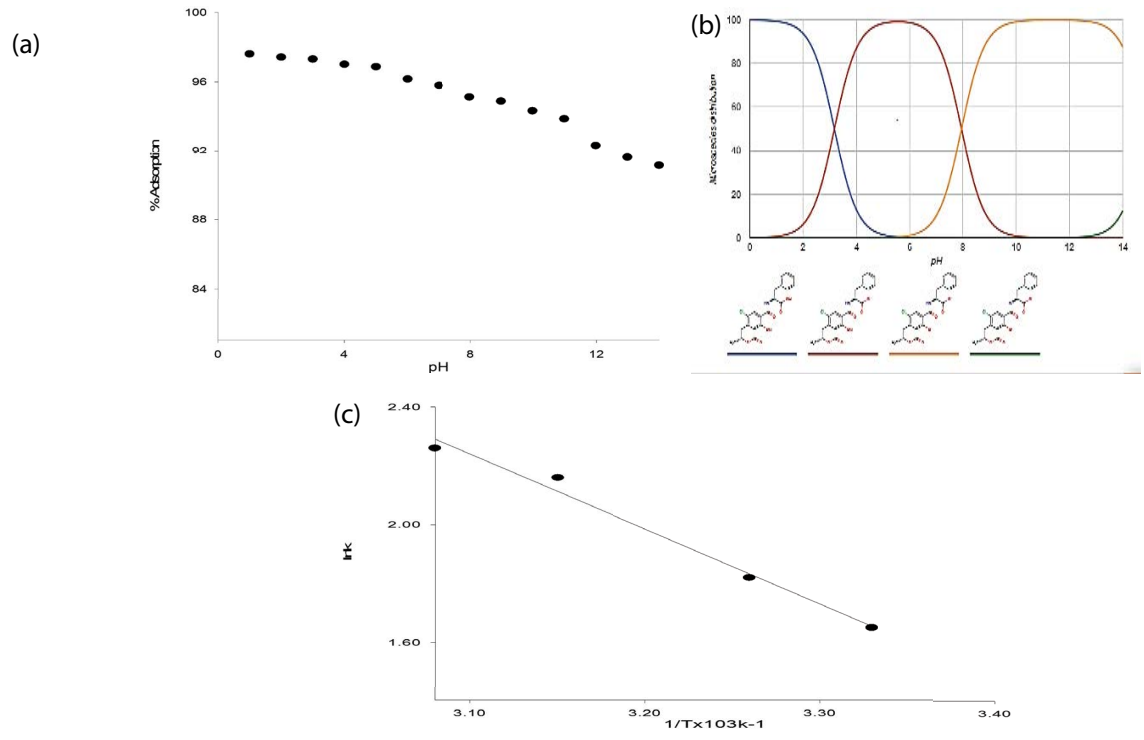

Fig. 3. Effect of pH and temperature on ochratoxin A adsorption. (a) Effect of pH, (b) micro species distribution diagram and (c) Van't Hoff plot.

4. Conclusion

A novel adsorbent, highly porous carbon nanocomposite, was prepared from sugar beet wastes and was used for the in vitro detoxification of ochratoxin A. The prepared adsorbent exhibited high adsorption capacity for the adsorption of ochratoxin A. The values of $\Delta H°$ (–21 kJ mol^{-1}) and $\Delta G°$ (–2.75, –3.57, –4.39 and –5.21 kJ mol^{-1} corresponding to temperatures 30°C, 40°C, 50°C and 60°C, respectively) were negative while that of $\Delta S°$ (85 kJ mol^{-1} deg^{-1}) was positive indicating the favorable nature of the process. The increased value of $\Delta G°$ with temperature demonstrated that the adsorption process was favorable at high temperature. From the results, it was concluded this adsorbent can be effectively used to remove OTA from solution. This adsorbent if mixed with poultry feed would effectively detoxify OTA produced by fungi.

References

[1] G.H.D. Van der Stegen, P.J.M. Essens, J. Van der Lijn, Effect of roasting conditions on reduction of ochratoxin A in coffee, J. Agric. Food Chem., 49 (2001) 4713–4715.

[2] P. Bucheli, M.H. Taniwaki, Research on the origin, and on the impact of post-harvest handling and manufacturing on the presence of ochratoxin A in coffee, Food Add. Cont., 19 (2002) 655–665.

[3] J. Varga, K. Rigo, B. Toth, J. Teren, Z. Kozakiewicz, Evolutionary relationships among *Aspergillus* species producing economically important mycotoxins, Food Technol. Biotechnol., 11 (2003) 29–36.

[4] M. Zahoor, F.A. Khan, Adsorption of aflatoxin B1 on magnetic carbon nanocomposites prepared from bagasse, Arab. J. Chem., 11 (2018) 729–738.

[5] I. Ali, Z.A. ALOthman, A. Al-Warthan, Sorption, kinetics and thermodynamics studies of atrazine herbicide removal from water using iron nano-composite material, Int. J. Environ. Sci. Technol., 13 (2016) 733–742.

[6] I. Ali, Z.A. ALOthman, A. Al-Warthan, Removal of secbumeton herbicide from water on composite nanoadsorbent, Desal. Wat. Treat., 57 (2016) 10409–10421.

[7] J. Stroka, E. Ankalam, U. Jorissen, J. Gilbert, Immunoaffinity column cleanup with liquid chromatography using post-column bromination for determination of aflatoxins in peanut butter, pistachio paste, fig past, paprika powder, a collaborative study, J. AOAC Int., 83 (2000) 320–340.

[8] M.M.U. Rahman, M. Zahoor, B. Muhammad, F.A. Khan, R. Ullah, N.M. AbdEI-Salam, Removal of heavy metals from drinking water by magnetic carbon nanostructures prepared from biomass, J. Nanomater., 2017 (2017) 1–10.

[9] F. Zhang, K.X. Wang, G.D. Li, J.S. Chen, Hierarchical porous carbon derived from rice straw for lithium ion batteries with high-rate performance, Electrochem. Commun., 11 (2009) 30–133.

[10] S. Krehula, S. Music, Formation of magnetite in highly alkaline media in the presence of small amounts of ruthenium, Croatia Chemica Acta, 80 (2007) 517–527.

[11] X. Liu, M. Kim, Solvothermal synthesis and magnetic properties of magnetic nano-platelets, Mater. Lett., 63 (2009) 428–430.

[12] Z. Al-Qodah1, R. Shawabkah, Production and characterization of granular activated sludge, Brazilian J. Chem. Eng., 26 (2009) 127–136.

[13] P. Hadi, M. Xu, C. Ning, C.S. Lin, G. McKay, A critical review on preparation, characterization and utilization of sludge-derived activated carbons for wastewater treatment, Chem. Eng. J., 260 (2015) 895–906.

[14] M. Sneha, N.M. Sundaram, Preparation and characterization of an iron oxide-hydroxyapatite nanocomposite for potential bone cancer therapy, Int. J. Nanomed., 10 (2015) 99–106.

[15] C.H. Giles, T.H. Macewan, S.N. Nakhwa, D. Smith, Studies in adsorption part IX: a system of classification of solution adsorption isotherms and its use in diagnosis of adsorption mechanism and its measurement of specific surface areas of solids, J. Am. Chem. Soc., 30 (1960) 3973–3993.

[16] I. Langmuir, The adsorption of gases on plane surfaces of glass mica and platinum, J. Am. Chem. Soc., 40 (1918) 1361–1403.

[17] U.U. Freundlich, Adsorption in solution, Z. Phys. Chem., 57 (1906) 384–470.

[18] M.I. Temkin, V. Pyzhev, Kinetics of ammonia synthesis on promoted iron catalyst, Acta Phys. Chim. USSR, 12 (1940) 327–356.

[19] Y.S. Ho, G. McKay, Sorption of dye from aqueous solution by peat, Chem. Eng. J., 70 (1998) 115–124.

[20] S. Lagergren, Zurtheorie der sogenannten adsorption geloesterstoffe, K. Sven. Vetensakad., Handl., 241 (1898) 1–39.